



T.C.
YÜKSEKÖĞRETİM KURULU BAŞKANLIĞI
ANKARA

05.03.2024

OKUL TANIMA BELGESİ

T.C. Kimlik No : 22520560338
Adı Soyadı : İLKAY DEMİR
Ülke : TUNUS
Üniversite : Faculté des Sciences de Sfax
Durumu : Kurulumuzda mevcut uluslararası listelerde yer almaktadır.

Açıklama

Yurtdışındaki yükseköğretim kurumlarından örgün eğitim yoluyla alınan diplomaların denklik işlemi, 2547 sayılı Yükseköğretim Kanunu'nun 2880 sayılı kanunla değişik 7/p maddesi ile 05.12.2017 tarihli Resmi Gazete'de yayımlanan "Yurtdışı Yükseköğretim Diplomaları Tanıma ve Denklik Yönetmeliği" hükümleri uyarınca yapılmakta olup, söz konusu Yönetmelik yatay geçiş, dikey geçiş ve lisans tamamlama gibi kavramları kapsamamaktadır.

Yurtdışındaki yükseköğretim kurumlarından uzaktan öğretim yoluyla alınacak diplomalar ise söz konusu Yönetmeliğin 10. maddesi ve ilgili mevzuat çerçevesinde değerlendirilmektedir.

Öğrenim dili Türkçe olan yurt dışındaki yükseköğretim programlarından alınan diplomalar için yapılan başvurular Yönetmelik'in 7. madde, 6. fıkra, (ç) bendi "*Türkiye'nin taraf olduğu uluslararası anlaşmalarla öğrenim dilinin Türkçe olduğu belirlenen programlar veya Yükseköğretim Kurulunca tanınan yurtdışındaki Türkçe yükseköğretim programları dışında, yükseköğretim kurumlarının açtığı ve öğrenim dili Türkçe olan programlardan alınan diplomalar için yapılan başvurular reddedilir.*" hükmü çerçevesinde karara bağlanacaktır.

Diploma denklik başvurusunda aranacak belgeler ile inceleme ve değerlendirme usul ve esasları Yurtdışı Yükseköğretim Diplomaları Tanıma ve Denklik Yönetmeliği'nde belirtilmiş olup; ilgili Yönetmelik ve detaylı bilgiye Yükseköğretim Kurulu web sayfasından ulaşılabilmektedir.

Yatay geçiş başvuruları, 08.02.2008 tarih ve 636/2732 sayılı yazımız ile "Yükseköğretim Kurumları Arasında Ön lisans ve Lisans Düzeyindeki Programlar Arasında Geçiş, Çift Anadal, Yan Dal ile Kurumlar Arası Kredi Transferi Yapılması Esaslarına İlişkin Yönetmelik" hükümlerine; lisansüstü eğitim başvuruları ise 26.09.2017 tarih ve 64528 sayılı yazı ile "Lisansüstü Eğitim ve Öğretim Yönetmeliği" hükümlerine uygun olarak, alınan dersler incelenmek suretiyle başvuru yapılan Üniversite tarafından değerlendirilmekte ve karara bağlanmaktadır.

2547 Sayılı Kanun'un 11 b/5 maddesi uyarınca yurtdışında yapılan doktora eğitimleri Üniversitelerarası Kurul tarafından değerlendirilmektedir. Yurtdışında yapılan doktora eğitiminin Türkiye'de yapılan doktora eşdeğer olup olmayacağı hususunda önceden herhangi bir görüş belirtmek mümkün olmadığı gibi, söz konusu eşdeğerlik, doktora tamamlandıktan sonra ilgili komisyon ve kurullar tarafından incelenmektedir.

Öte yandan diploma denklik başvuruları, ilgili Komisyon ve Kurullar tarafından münferiden değerlendirildiğinden yurt dışındaki yükseköğretim kurumlarından alınmış ön lisans, lisans ve yüksek lisans diplomalarının ülkemizdeki diplomalara eşdeğer olup olmayacağı hususunda önceden herhangi bir görüş belirtmek mümkün olmadığı gibi, eğitim alınan yükseköğretim kurumunun tanınırlığına ilişkin olarak Kurulumuzun yeni kararlar alma hakkı saklıdır.

Yurt dışında yükseköğrenim görmek isteyen öğrencilerin konuyla ilgili güncel gelişme ve kararları Kurulumuz internet adresinden takip etmeleri yararlarına olacaktır.

Bilgilerinizi rica ederim.

***BU BELGE DENKLİK BELGESİ YERİNE GEÇMEZ**

Bu belgenin doğruluğunu barkod numarası ile <https://www.turkiye.gov.tr/belge-dogrulama> adresinden, mobil cihazlarınıza yükleyeceğiniz e-Devlet Kapısına ait Barkodlu Belge Doğrulama veya YÖK Mobil uygulaması vasıtası ile yandaki karekod okutularak kontrol edilebilir.



JOURNAL OF MOLECULAR STRUCTURE

Publisher name: ELSEVIER

Journal Impact Factor™

3.8

2022

3.2

Five Year

JCR Category	Category Rank	Category Quartile
CHEMISTRY, PHYSICAL <i>in SCIE edition</i>	74/161	Q2

Source: Journal Citation Reports 2022. [Learn more](#)

Journal Citation Indicator™

0.57

2022

0.52

2021

JCI Category	Category Rank	Category Quartile
CHEMISTRY, PHYSICAL <i>in SCIE edition</i>	89/172	Q3

The Journal Citation Indicator is a measure of the average Category Normalized Citation Impact (CNCI) of citable items (articles and reviews) published by a journal over a recent three year period. It is used to help you evaluate journals based on other metrics besides the Journal Impact Factor (JIF).

[Learn more](#)

Interested in reviewing for this journal?

Add this journal to your reviewer interest list. [Add Journal](#)

Full text at publisher



Export

Add To Marked List



Comprehensive growth and characterization study of GeOx/Si

By Baghdedi, D (Baghdedi, Dhouha) ^{[1], [2], [3]}; Hopoglu, H (Hopoglu, Hicret) ^{[2], [3]}; Saritas, S (Saritas, Sevda) ^[4]; Demir, I (Demir, Ilkay) ^{[3], [5]}; Altuntas, I (Altuntas, Ismail) ^{[3], [5]}; Abdelmoula, N (Abdelmoula, Najmeddine) ^[1]; Gür, E (Gur, Emre) ^[6]; Tüzemen, ES (Tuzemen, Ebru Senadim) ^{[2], [3]}

[View Web of Science ResearcherID and ORCID](#) (provided by Clarivate)

Source JOURNAL OF MOLECULAR STRUCTURE

Volume: 1274 Part: 1

DOI: 10.1016/j.molstruc.2022.134398

Article Number 134398

Published FEB 15 2023

Early Access OCT 2022

Indexed 2023-01-23

Document Type Article

Abstract In this study, the reactive radio frequency magnetron sputtering (RFMS) method under varying thickness was used to deposit GeOx on Si substrate at room temperature. The effect of thickness on the structural and optical properties of high-quality germanium dioxide (GeO₂) thin films have been investigated by experimental. Structural properties were investigated using X-ray diffraction. It has been observed that the peak intensity of (113) reflection is the highest in the spectrum of 240.22 nm thickness and using scanning electron microscope (SEM) to calculate thickness of different samples. Reflection measurement, which is one of its optical properties, was measured with an optical spectrophotometer. It has been observed that as the thickness increases, the total reflectance changes. The absorption coefficient was calculated using the diffuse reflection curve. From this point of view, the energy band gap was calculated and it was seen that it varies between 4.1 eV and 4.4 eV. As a result, it was observed that the energy band gap increased as the thickness increased. And using spectroscopic ellipsometry to calculate the thickness of different, refractive index, extinction coefficient, and oscillator parameters. The oscillator energy decrease as the thickness of films increases

Citation Network

In Web of Science Core Colle

1 Citation

[Create citation alert](#)

1 Times Cited in All Data

[+ See more times cited](#)

25 Cited References

[View Related Records](#) →

Citing items by classifica

Breakdown of how this article is mentioned, based on available context data and snippets from citing item(s).

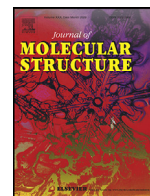
Background 0

Basis 0

Support 0

Differ 0

Discuss 0



Comprehensive growth and characterization study of GeO_x/Si

Dhouha Baghdedi^{a,b,c}, Hicret Hopoğlu^{b,c}, Sevda Sarıtaş^d, İlkay Demir^{c,e}, İsmail Altuntaş^{c,e}, Najmeddine Abdelmoula^a, Emre Gür^f, Ebru Şenadım Tüzemen^{b,c,*}

^a Laboratory of Multifunctional Materials and Applications (LaMMA), Faculty of Sciences of Sfax, University of Sfax, Tunisia

^b Department of Physics, Sivas Cumhuriyet University, Sivas 58140, Turkey

^c Nanophotonics Research and Application Center, Sivas Cumhuriyet University, Sivas 58140, Turkey

^d İspir Hamza Polat Vocational School, Ataturk University, Erzurum, Turkey

^e Department of Nanotechnology Engineering, Sivas Cumhuriyet University, Sivas 58140, Turkey

^f Department of Physics, Faculty of Science, Ataturk University, Erzurum 25240, Turkey

ARTICLE INFO

Article history:

Received 26 July 2022

Revised 6 October 2022

Accepted 20 October 2022

Available online 22 October 2022

Keywords:

GeO_x

Magnetron sputtering

Optical properties

Structural properties

ABSTRACT

In this study, the reactive radio frequency magnetron sputtering (RFMS) method under varying thickness was used to deposit GeO_x on Si substrate at room temperature. The effect of thickness on the structural and optical properties of high-quality germanium dioxide (GeO₂) thin films have been investigated by experimental. Structural properties were investigated using X-ray diffraction. It has been observed that the peak intensity of (113) reflection is the highest in the spectrum of 240.22 nm thickness and using scanning electron microscope (SEM) to calculate thickness of different samples. Reflection measurement, which is one of its optical properties, was measured with an optical spectrophotometer. It has been observed that as the thickness increases, the total reflectance changes. The absorption coefficient was calculated using the diffuse reflection curve. From this point of view, the energy band gap was calculated and it was seen that it varies between 4.1 eV and 4.4 eV. As a result, it was observed that the energy band gap increased as the thickness increased. And using spectroscopic ellipsometry to calculate the thickness of different, refractive index, extinction coefficient, and oscillator parameters. The oscillator energy decrease as the thickness of films increases and the dispersion energy increase with the increase of thickness. It has been observed that the thickness varies between 174.29 nm and 332.16 nm. The refractive index increases as the thickness increases.

© 2022 Published by Elsevier B.V.

1. Introduction

In recent years, semiconductor thin films have aroused great interest because of their outstanding properties. Germanium dioxide (GeO₂) has special optical and electrical properties. Besides, it has attracted the attention of researchers because of its potential applications in modern nanoscale electronic and optical devices [1–3]. In addition, GeO₂ is a promising material that shows interesting properties. Having a higher refractive index slightly higher than silicon, GeO₂ is thermally stable. It is also a material with high transmittance, wide optical band gap (>5 eV), good mechanical strength, high dielectric constant, and high carrier mobility [1–3]. These interesting properties of GeO₂ make it useful in many domains like optoelectronics [4–6], memory application [7], as a host the material in luminescent devices [8], optical applications (opti-

cal storage applications and optical waveguides) [4], potential anode materials for high-energy Li-ion batteries [9] and in photodetector [10].

The properties of GeO₂ thin films strongly depend on the deposition parameters. Various methods of depositing of GeO₂ that have been adopted by the researchers for the growth of GeO₂ thin films including radio frequency RF magnetron sputtering [4], laser ablation, liquid phase deposition, [11] and the other techniques [12].

The CO₂ laser irradiation of GeO₂ planar waveguide fabricated by RF-sputtering has been studied by Chiasera A. et al. [4]. In this study, the researchers deposited GeO₂ transparent glass-ceramic planar waveguides with the RF sputtering technique and then irradiated them with a pulsed CO₂ laser. Using different techniques such as micro-Raman spectroscopy, atomic force microscopy, and positron annihilation spectroscopy for structural effects, they gained knowledge about the structural changes produced after irradiation in waveguide films with a thickness of about 1 μm.

* Corresponding author at: Department of Physics, Sivas Cumhuriyet University, Sivas 58140, Turkey.

E-mail address: esenadim@cumhuriyet.edu.tr (E.Ş. Tüzemen).

The evaluation of lattice dynamics, infrared optical properties, and visible emissions of hexagonal GeO_2 films prepared by liquid phase deposition are studied by Yabin Sun et al. [11]. In this study, the researchers deposited films with a thickness of 10 to 22 μm on Si(100) substrate using liquid phase deposition. The effects of crystallographic and vibrational properties and optical properties, X-ray diffraction (XRD), scanning electron microscopy, Raman scattering and infrared (IR) reflection/transmittance, and the effects of deposition time on thickness were investigated.

Ion-beam modification of the structural and optical properties of GeO_2 thin films grown using pulsed laser deposition at various substrate temperatures was investigated by Mahendra Singh Rathore et al. [12]. They irradiated the grown films with 100 MeV Ag^{7+} ions at a constant flow of 1×10^{13} ions/cm² and characterized using X-ray diffraction, atomic force microscopy, Raman spectroscopy, Fourier transform, infrared and photoluminescence spectroscopy.

It is also reported that the synthesis and characterization of GeO_2 thin films prepared by e-beam evaporation have been investigated by Mahendra Singh Rathore et al. [13]. GeO_2 thin films were deposited on silicon (100) substrate at 150°C using e-beam evaporation. These as-deposited films were annealed at various temperatures ranging from 600° to 800°C for an hour in an air atmosphere. The surface morphology of as-deposited and annealed films was studied using (AFM). The different vibration modes of GeO_2 were investigated by FTIR spectroscopy. The functional group and different optical phonon modes configuration were analyzed by Raman spectroscopy.

Following the literature review, when we examine the most recent situation concerning the GeO_2 semiconductor oxide material, it is seen as a shortcoming that this material has not been extensively studied on the RF magnetron sputtering method.

The present work concentrates on the performing comprehensive growth and optical and structural characterization of GeO_2 thin films, grown by RF magnetron sputtering deposition method with a variety of thickness at room temperature, on p-Si substrate. Studies were made to understand the effect of the thickness on the structural and optical properties of these many GeO_2 thin films. The results obtained are presented and discussed in this paper.

2. Experimental details

GeO_x thin films were deposited by using reactive RF magnetron sputtering method varying thickness on p-Si substrate. NANOVAK NVT5-400-2TH2SP Thermal & Sputter combined System was used for material deposition. Deposition parameters of the films grown are argon gas 92%, O_2 8% base pressure 8.3×10^{-6} Torr, working pressure 13×10^{-3} Torr, power 60 W and rotate 10 rpm. The crystal structure of GeO_x were analyzed using X-Ray Diffraction (XRD) technique and using scanning electron microscope (SEM). The optical properties of the grown samples were examined by optical spectrophotometer and spectroscopic ellipsometry. Reflectance spectra were obtained by spectrophotometer measurements and the effect of thickness was investigated. By using the diffuse reflectance curve, the absorption coefficient and then the energy band gap has been calculated with Kubelka Munk method. Optical constants were obtained by using spectroscopic ellipsometry. The spectral dependencies of refractive index, extinction coefficient, and complex dielectric function were revealed by analyzing experimental ellipsometric data under the light of the sample-air optical model. The thickness found from the spectroscopic ellipsometer and the thickness found from the SEM measurement were compared. At the same time, single oscillator energy and dispersion energy were calculated for GeO_x /Si structures using the Wemple-DiDomenico single oscillator model (WDD) [14–16].

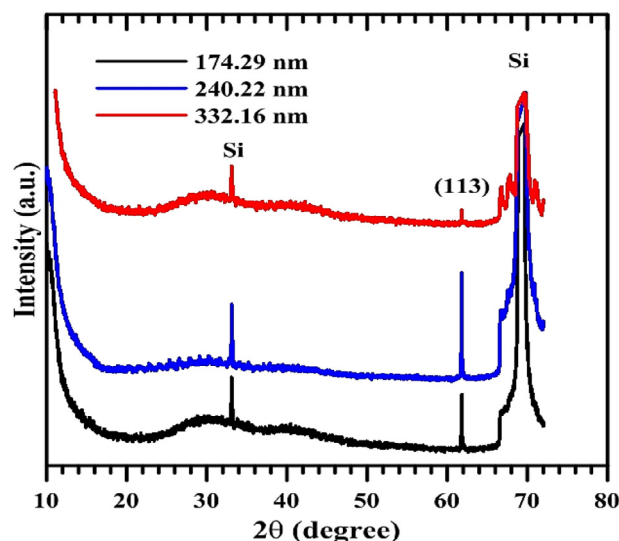


Fig. 1. XRD plot of GeO_x thin films produced on silicon at different thicknesses.

Table 1

X-ray diffraction data summary of GeO_2 thin films with different film thicknesses grown by RF Magnetron Sputtering.

Film thickness	174.29 nm	240.22 nm	332.16 nm
2θ (°)	61.82	61.79	61.82
FWHM (°)	0.0875	0.0812	0.1183
Grain size (nm)	106.28	114.56	78.42
d (nm)	0.1499	0.1496	0.1498

3. Results and discussion

3.1. Structural characterization

3.1.1. X-Ray Diffraction (XRD) technique

X-ray diffraction patterns of GeO_x thin films produced in different thicknesses on silicon substrates were measured by PANalytical EMPYREAN XRD model X-ray spectrometer. The XRD patterns of the GeO_x films grown are shown in Fig. 1. Three peaks were observed in all films. Two of these peaks belong to the silicon substrate. These peaks belong to (100) and (400) planes. Only one peak was observed for GeO_x . This peak is around 62° and belongs to the (113) orientation [17–19]. The intensity of (113) is the highest in the spectrum of 240.22 nm thickness.

In Table 1, full width at half maximum (FWHM), grain size, and interplanar distances (d) of 174.29 nm, 240.22 nm, and 332.16 nm films are calculated. As seen in Table 1, the FWHM of the peak (113) of the 240.22 nm film is narrower than the other samples. Accordingly, the grain size is larger than the others.

3.1.2. Scanning electron microscope (SEM)

SEM measurement was taken from the cross-section of the sample and only the thickness was measured. The thicknesses of the films were found to be approximately ~164.89 nm, ~240.60 nm, and ~318.98 nm respectively. SEM analyses were performed at 10 kV with a working distance of 11.35 mm for 164.89 nm, 10.57 mm for 240.60 nm, and 9.95 mm for 318.98 nm at 500 nm are shown in Fig. 2(a–c).

3.2. Optical characterization

3.2.1. Optical spectrophotometer

Reflection measurements of GeO_x thin films produced in different thicknesses on Si (100) substrate were made using Varian Cary

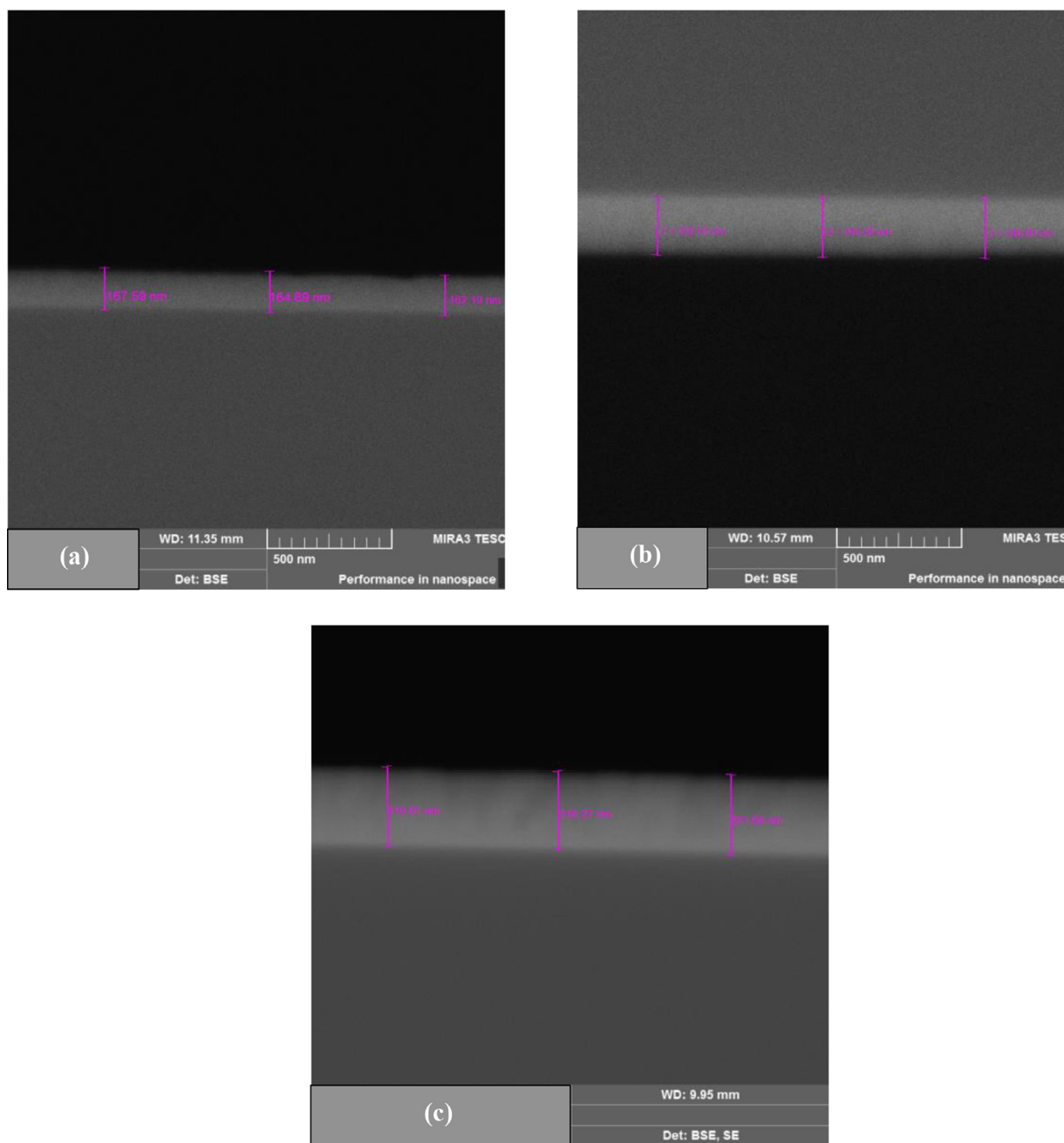


Fig. 2. SEM results of GeO_x thin films at different thicknesses (a) 164.89 nm, (b) 240.60 nm, (c) 318.98 nm.

5000 model UV–Vis–NIR spectrophotometer and PTFE as reference disc. Total reflection spectra were taken in the range of 200–1200 nm in the air at room temperature, and diffuse reflection spectra were taken in the range of 200–800 nm.

In this study, the Kubelka–Munk function was used to calculate the absorption coefficient. When using the Kubelka–Munk function, diffuse reflection spectra are used. The Kubelka–Munk theory helped us find the energy band gap of thin films on opaque substrates. Diffuse reflectance data (R) was calculated using Kubelka–Munk function by the relation [20]:

$$F(R) = \frac{(1 - R)^2}{2R} = \frac{K}{s} \quad (1)$$

In Eq. (1), F(R) is the Kubelka–Munk function corresponding to the absorption, K is the absorption coefficient and s is the scattering coefficient. The absorption coefficient of a direct bandgap semi-

conductor is expressed by the Tauc equation [21,22]:

$$\alpha h\nu = A(h\nu - E_g)^n \quad (2)$$

In Eq. (2), α is the material's linear absorption coefficient, $h\nu$ is the photon energy, A is the proportionality constant, and n is a constant describing the optical transition type. The Kubelka–Munk function is directly proportional to the absorption coefficient.

$$\alpha = \frac{F(R)}{t} \quad (3)$$

where t is the thickness of film [20].

Fig. 3(a) shows the total reflectance spectra of GeO₂ thin films at different thicknesses at room temperature in the wavelength range of 200–1200 nm. Multiple peaks in Fig. 3(a) represent interference fringes. Since this study is dependent on the film thickness, the number of interference fringe peaks increases as the film thickness increases.

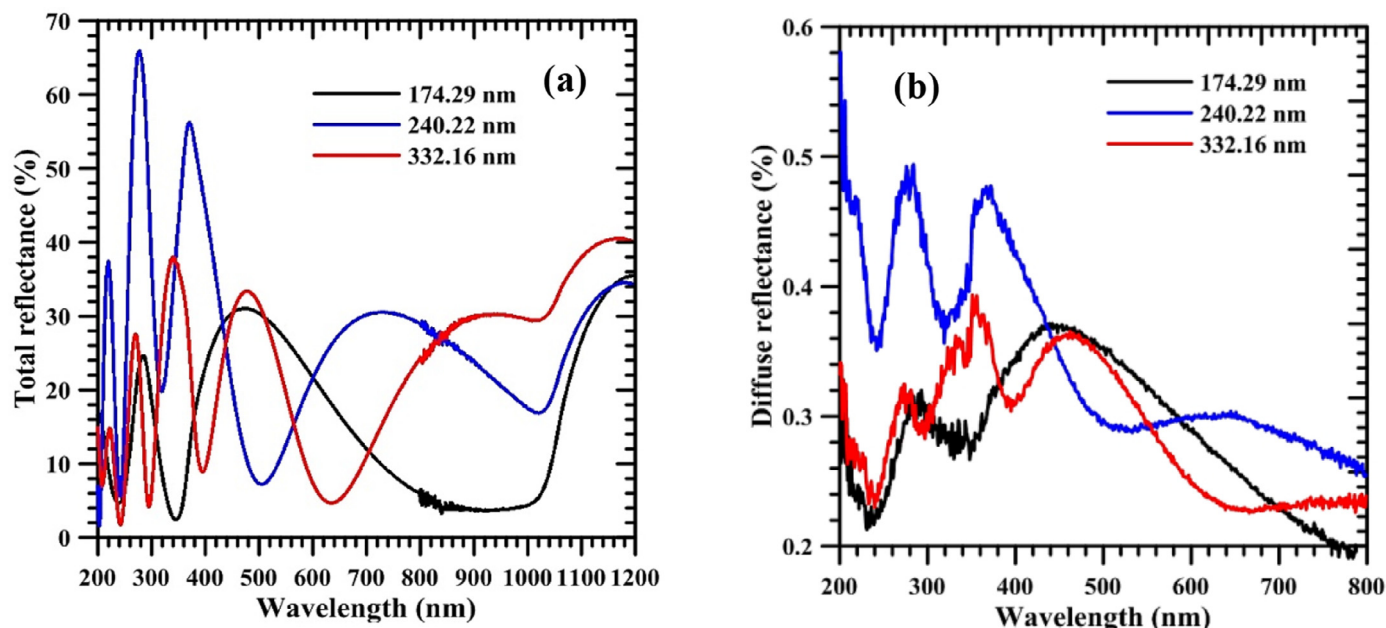


Fig. 3. (a) Total reflectance spectra of GeO_2 thin films on p-Si substrate with different thicknesses, (b) Diffuse reflectance spectra of GeO_x thin films on p-Si substrate with different thicknesses.

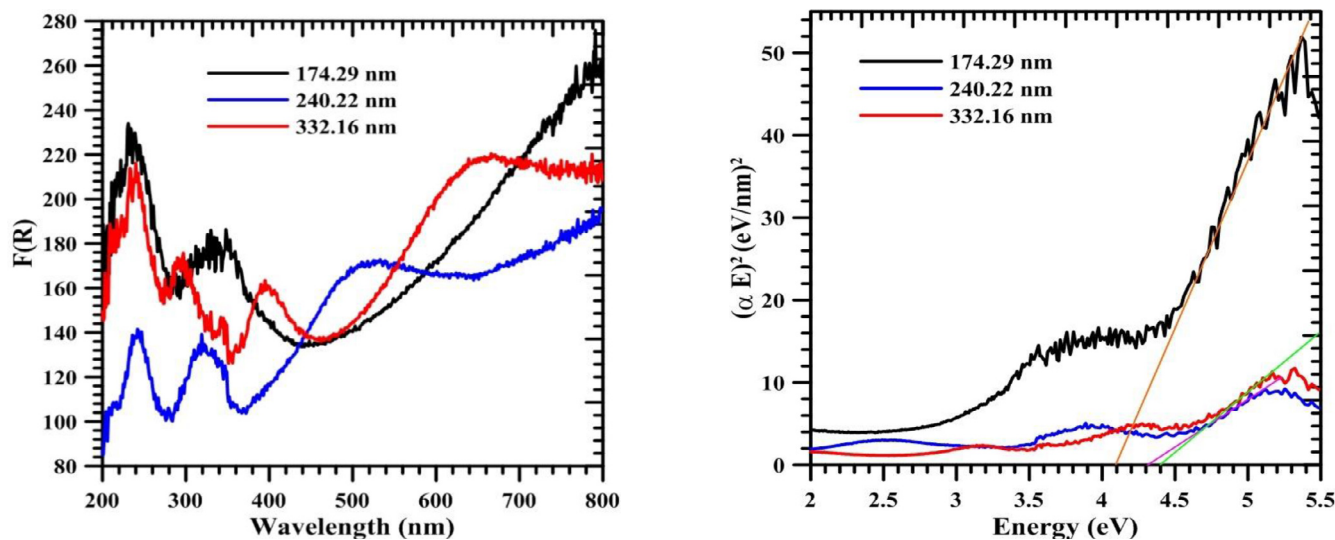


Fig. 4. $F(R)$ versus wavelength.

Fig. 5. $(\alpha E)^2$ spectra of GeO_x thin films on p-Si substrate with different thicknesses.

According to total reflectance spectra, there are two absorption edges. One belongs to GeO_x and the other belongs to silicon. It is seen that the sharpness of the absorption edge of silicon decreases as the thickness decreases from the absorption region of silicon, which is around 1000 nm. As the thickness decreases, the absorption edge shifts towards the infrared region. Fig. 3(b) shows the diffuse reflectance spectra of GeO_x thin films at different thicknesses at room temperature in the wavelength range of 200–800 nm. Diffuse reflection measurement is essential for us to find the energy band gap. The diffuse reflection in Eq. (1) was used to find $F(R)$. Fig. 4 shows the change in $F(R)$ in the Kubelka Munk formula for thin films with different thicknesses.

According to the graph of $F(R)$ versus wavelength values (Fig. 4), the UV-absorption edge of 174.29 nm was around 240–290 nm, the UV-absorption edge of 240.22 nm was around 243–280 nm and the UV-absorption edge of 332.16 nm was around 243–275 nm. It has

Table 2

Energy band gap of GeO_x thin films on p-Si substrate with different thicknesses.

Thickness (nm)	Substrate temperature (°C)	Energy band gap (eV)
174.29	RT	4.1
240.22	RT	4.3
332.16	RT	4.4

been observed that as the thickness increases, the UV-absorption edge decreases in energy units.

In this study, the energy band gap of GeO_x films was calculated by plotting the square of the Kubelka-Munk function with respect to energy. The value of the linear part of the curve on the energy axis gives us the energy band gap of the films in Fig. 5. The corresponding values of E_g have been given in Table 2.

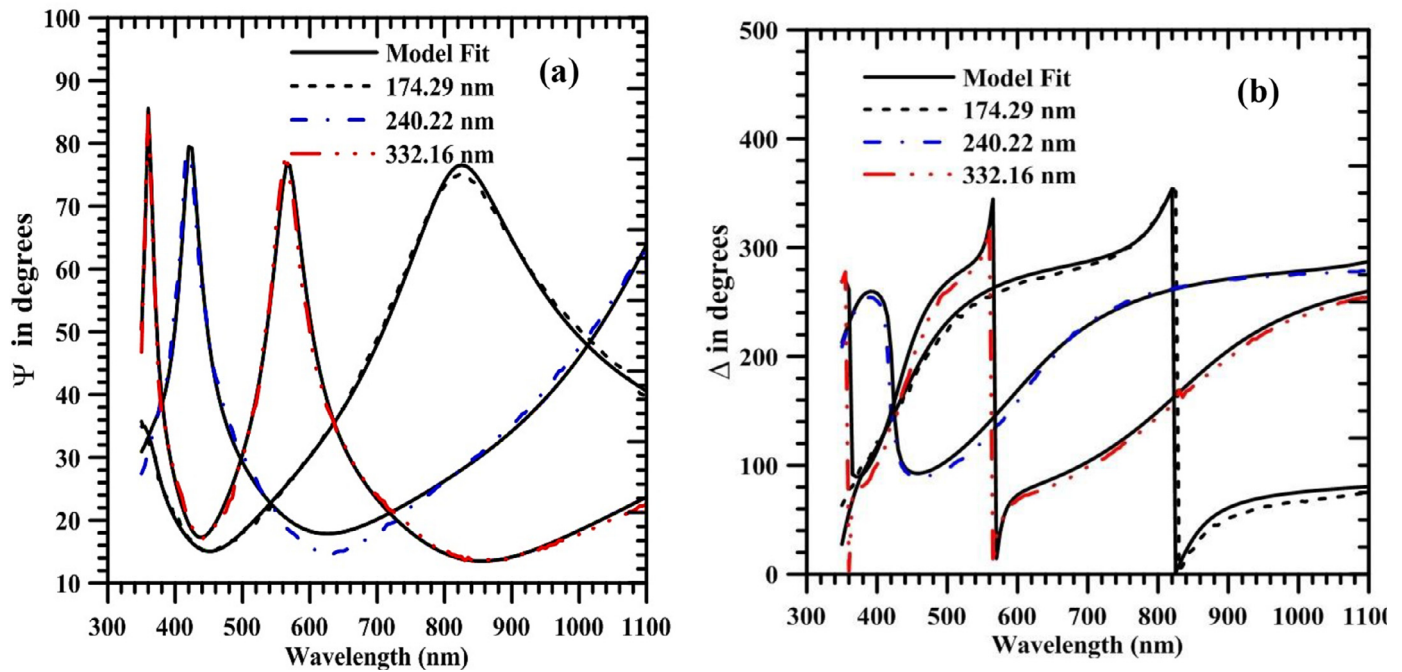


Fig. 6. (a) The spectral dependence of Ψ for 174.29 nm, 240.22 nm and 332.16 nm, (b) The spectral dependence of Δ for 174.29 nm, 240.22 nm and 332.16 nm.

It has been observed that as the thickness increases, the energy band gap increases from 4.1 eV to 4.4 eV. Band gap and optical properties show a strong dependence on film thickness. The variation of the energy band gap with the change of film thickness is related to the density of localized states. Therefore, since the energy band gap increases, the density of localized states is low.

3.2.2. Spectroscopic ellipsometry

Spectroscopic ellipsometry technique was used to carry out the optical analysis in more detail, and the OPT-S9000 Ellipsometer device was used for this. The thickness of the films, refractive index, extinction coefficient, dielectric constant, and oscillator parameters were obtained by the ellipsometry technique. The complex reflection ratio in the spectroscopic ellipsometry technique can be defined as follows [22–24]:

$$\rho = \frac{\tilde{R}_p}{\tilde{R}_s} = \tan\psi e^{i\Delta} \quad (4)$$

Here, ρ shows the ratio of the complex reflection coefficient, which is polarized parallel to the incidence plane \tilde{R}_p , and the complex reflection coefficient which is polarized perpendicular to the incidence plane \tilde{R}_s . The ratio of \tilde{R}_p to \tilde{R}_s gives the expression of the ellipsometric Ψ parameter:

$$\tan\psi = \frac{R_p}{R_s} \quad (5)$$

The phase difference between R_p and R_s gives another ellipsometric parameter Δ :

$$\Delta = \Delta_p - \Delta_s \quad (6)$$

Here, Δ_p and Δ_s are the phases of R_p and R_s , respectively.

In this study, the measurements were made in the wavelength range of 350–1100 nm with a step size of 5 nm and with an angle of incidence 65° . After measurements, the data were analyzed for determining the refractive index, extinction coefficient, oscillator parameters, and film thickness. For the calculation of the measurements, Cauchy model was used [22]. Cauchy model can be described as follows [22,23]:

$$n = n_\infty + \frac{A}{\lambda^2} + \frac{B}{\lambda^4} + \dots \quad (7)$$

Fig. 6(a) and 6(b) show the theoretical and experimental representative measurements of all samples of spectroscopic ψ and Δ according to wavelength respectively. As can be seen from both graphs, the fit is quite good and the MSE values are between 5 and 10.

The refractive indices of GeO_x films were determined by using the Ψ spectra where the correlation between the theoretical model and experimental data was fit the best.

The variation of refractive index of GeO_x films grown under different thicknesses and with silicon substrate is shown in the Fig. 7(a).

The refractive index is directly related to the internal structure of a film under investigation. As can be seen from the Fig. 7(a), the refractive index increases as the thickness increases. We can say that the orientation of the grains changed as the thickness increased.

The variation of the extinction coefficient of GeO_x films grown under different thicknesses and with silicon substrate are shown in the Fig. 7(b). As a result of the fit, the thicknesses were found to be 174.29, 240.22, and 332.16 nm, respectively.

Moreover, the complex dielectric constant of a solid is given as:

$$\hat{\epsilon}(\lambda) = \epsilon_1(\lambda) + i\epsilon_2(\lambda) \quad (8)$$

Here, real and imaginary parts are related to $n(\lambda)$ and $k(\lambda)$ as:

$$\epsilon_1(\lambda) = n^2(\lambda) - k^2(\lambda) \quad (9)$$

$$\epsilon_2(\lambda) = 2n(\lambda)k(\lambda) \quad (10)$$

The real part of the dielectric function $\epsilon_1(\lambda)$ was determined employing the Eq. (9) and a plot of $\epsilon_1(\lambda)$ as a function of wavelength is shown in Fig. 8(a).

As can be seen from Fig. 8(b), it is seen that the real part of the dielectric constant decreases with increasing wavelength in the visible region. The imaginary part of the dielectric function is determined using Eq. (10). The variation of the imaginary part of the dielectric function with respect to wavelength for films produced in different thicknesses is shown in Fig. 9. As can be seen from the

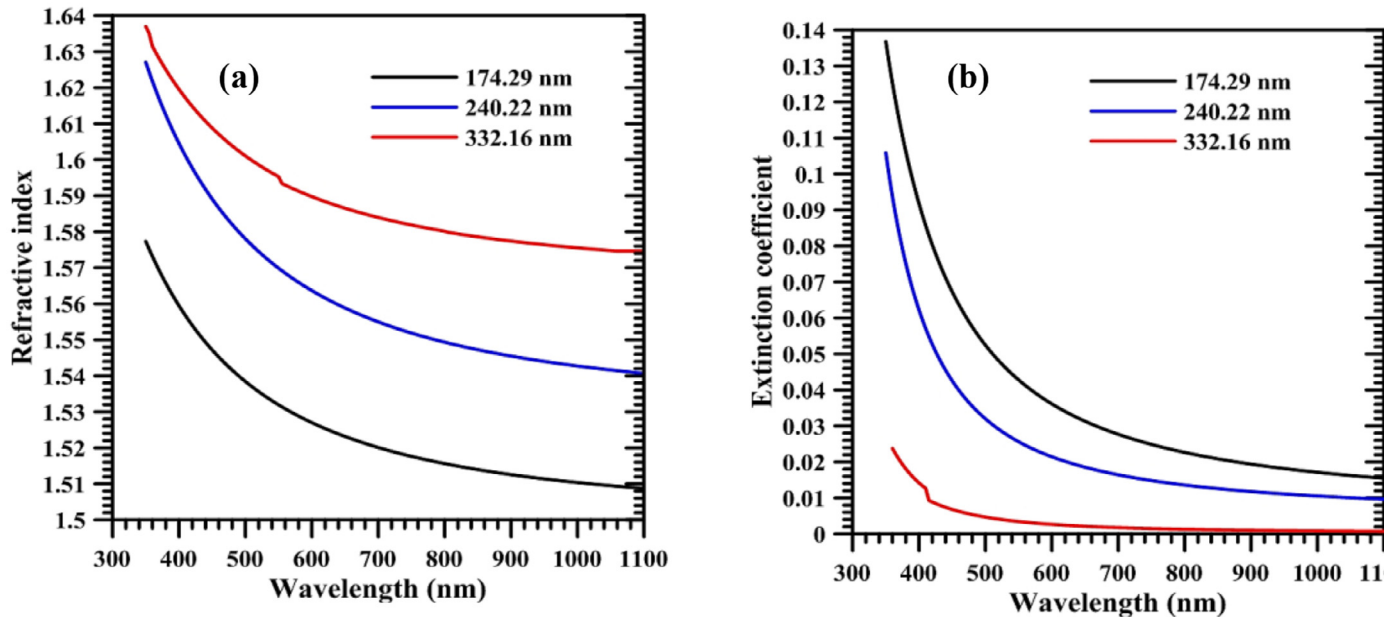


Fig. 7. (a) Dependence of the refractive index (n) with wavelength for different thicknesses of GeO_x thin films, (b) Dependence of the extinction coefficient (k) with wavelength for different thicknesses of GeO_x thin films.

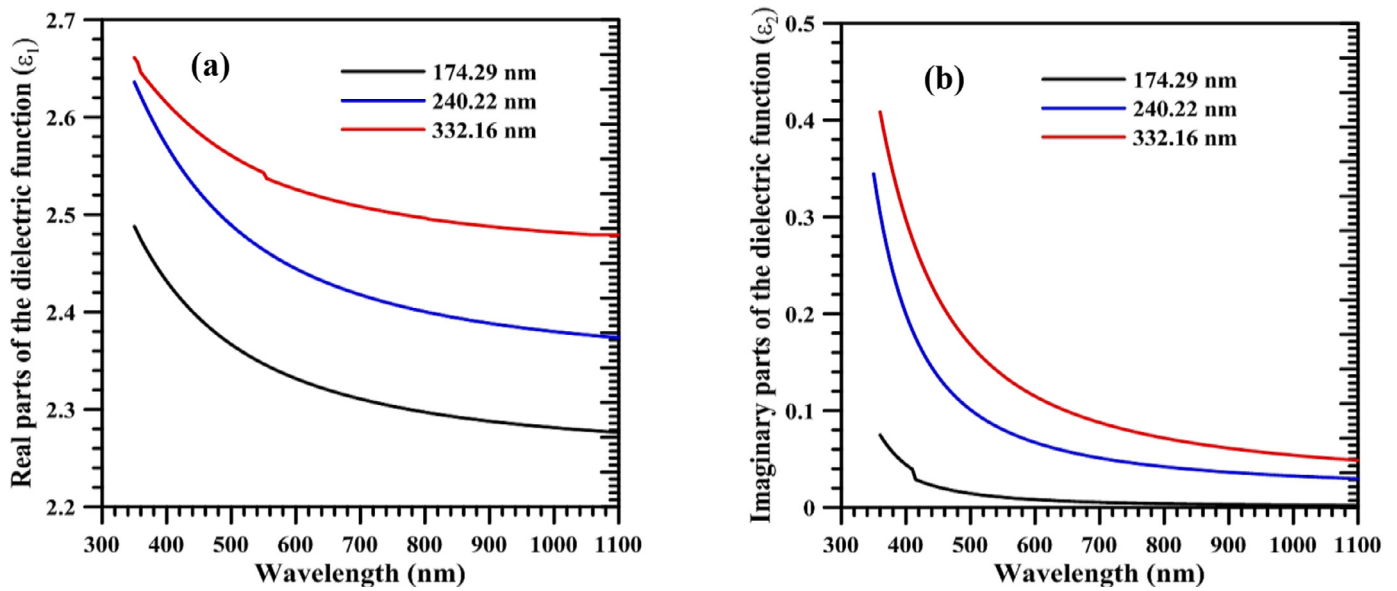


Fig. 8. (a) Real parts(ε₁) of the dielectric function as function of the wavelength for different thicknesses of GeO_x thin films, (b) Imaginary parts(ε₂) of the dielectric function as function of the wavelength for different thicknesses of GeO_x thin films.

figure, we can say that the dielectric constant is compatible with the literature [24].

In this study, the refractive index dispersion has been analyzed using the single-oscillator model developed by Wemple and DiDomenico [14–16]. According to this model, the relation between the refractive index n and photon energy E can be written as follows:

$$n = \left[1 + \frac{E_{osc}E_d}{E_{osc}^2 - (E^2)} \right]^2 \quad (11)$$

Where E_{osc} is the single-oscillator energy and E_d the dispersion energy. From equation E_{osc} and E_d can be obtained by plotting (n² - 1)⁻¹ against E².

From Fig. 9, the equations for the best fitting straight line are given as:

$$\text{For 174.29 nm : } \frac{1}{(n^2-1)} = -111,5 \times 10^{-4}E^2 + 0,797$$

$$\text{For 240.22 nm : } \frac{1}{(n^2-1)} = -119 \times 10^{-4}E^2 + 0,743$$

$$\text{For 332.16 nm : } \frac{1}{(n^2-1)} = -72,43 \times 10^{-4}E^2 + 0,685$$

Oscillator parameters E_d and E_{osc} are obtained from the intercepts and the slopes of the lines in the plot. These values have been listed in Table 3.

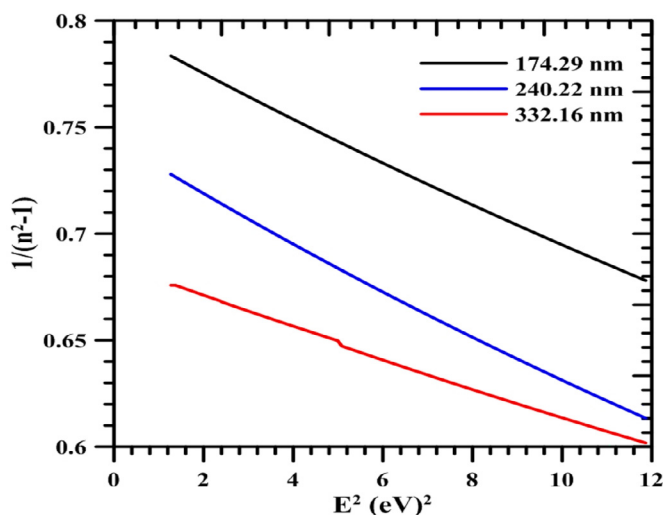


Fig. 9. Plot of $(n^2 - 1)^{-1}$ versus photon energy squared for different thicknesses of GeO_2 thin films.

Table 3
Oscillator parameters of GeO_2 thin films with different film thicknesses.

Samples Thicknesses	E_d (eV)	E_{osc} (eV)	E_g (eV)
174.29 nm	10.606	8.453	4.1
240.22 nm	10.63	7.901	4.3
332.16 nm	14.19	9.723	4.4

The refractive index of the incident photon, dispersion energy, average oscillator energy, and energy are parameters that are directly related to the internal structure of a film [25]. The dispersion energy (E_d) is related to the electronic oscillator power and the average oscillatory energy (E_{osc}) is related to the oscillator energy and consequently the average energy band gap of the studied film. Evidently, the value of E_{osc} of the GeO_x films increase as the thickness of films increases, which is expected because it is related directly to the average band gap of the studied film, by an empirical relation of the form $E_{osc} \sim 2E_g$.

As a result, it was revealed that there is a strong correlation between the chemical structural changes (lattice constant, chemical bonds, etc.) of the nanocrystalline GeO_x films deposited with E_d . Therefore, we can say that the increase in E_d as the thickness of the films increases is related to the increase in the lattice parameters.

4. Conclusions

In summary, the GeO_x films were successfully deposited on silicon substrates by reactive RF magnetron sputtering using germanium target by various thicknesses. The effect of film thickness on structural and optical properties was investigated. When the structural properties were examined, one peak was observed in the (113) orientation of GeO_x . The energy band gap of films can be calculated by plotting the square of the Kubelka–Munk function versus energy. It has been observed that as the thickness increases, the energy band gap increases from 4.1 eV to 4.4 eV. The ellipsometry measurements were made in the wavelength range of 350–1100 nm with a step size of 5 nm and with an angle of incidence 65° . The Cauchy model was used which is an optical model that is widely used in ellipsometric data analysis. As a result, it was observed that the refractive index increased as the thickness increased. It was observed that the film thicknesses found by SEM analysis and spectroscopic ellipsometry were quite close to each

other. The real part of the dielectric constant decreased with increasing wavelength in the visible region. In the normal dispersion region, the refractive index dispersion has been analyzed using the single-oscillator model developed by Wemple and DiDomenico.

CRediT authorship contribution statement

Dhouha Baghdedi Sample preparation and experiments, optical measurements, Writing original draft, Visualization. **Hicret Hopoğlu** Sample preparation and experiments. **Sevda Sarıtaş** X-ray data collection. **İlkay Demir** Writing original draft & review, optical measurements. **İsmail Altuntaş** Writing original draft, optical measurements. **Najmeddine Abdelmoula** Methodology, Writing review & editing. **Emre Gür** Methodology, Writing review & editing, X-ray data collection. **Ebru Şenadım Tüzemen** Methodology, Writing original draft, Writing review & editing, Investigation, Visualization.

Declaration of Competing Interest

The authors declare that they have no known competing financial interests or personal relationships that could have appeared to influence the work reported in this paper.

Data Availability

The authors do not have permission to share data.

Acknowledgments

This study is conducted in Sivas Cumhuriyet University R & D Center (CUTAM), Sivas Cumhuriyet University Nanophotonic Application and Research Center.

References

- [1] M.S. Rathore, A. Vinod, R. Angalakurthi, A.P. Pathak, S.K. Thatikonda, S.R. Nelamarri, Role of oxygen pressure on the structural and photoluminescence properties of pulsed laser deposited GeO_2 thin films, *Physica B: Condensed Matter* 625 (2022) 413466.
- [2] N.R. Murphy, J.T. Grant, L. Sun, J.G. Jones, R. Jakubiak, V. Shutthanandan, C.V. Ramana, Correlation between optical properties and chemical composition of sputter-deposited germanium oxide (GeO_x) films, *Opt. Mater.* 36 (2014) 1177–1182.
- [3] J.W. Miller, M. Chesaux, D. Deligiannis, P. Mascher, J.D.B. Bradley, Low-loss GeO_2 thin films deposited by ion-assisted alternating current reactive sputtering for waveguide applications, *Thin Solid Films* 709 (2020) 138165.
- [4] A. Chiasera, C. Macchi, S. Mariazzi, S. Valligatla, S. Varas, M. Mazzola, N. Bazzanella, L. Lunelli, C. Pederzoli, D.N. Rao, G.C. Righini, A. Somoza, R.S. Brusa, M. Ferrari, CO_2 Laser irradiation of GeO_2 planar waveguide fabricated by RF-sputtering, *Optical Components and Materials* 73 (2015) 012006.
- [5] M. Peng, Y. Li, J. Gao, D. Zhang, Z. Jiang, X. Sun, Electronic Structure and Photoluminescence Origin of Single-Crystalline Germanium Oxide Nanowires with Green Light Emission, *J. Phys. Chem. C* 115 (2011) 11420–11426.
- [6] H.W. Kim, S.H. Shim, J.W. Lee, Cone-shaped structures of GeO_2 fabricated by a thermal evaporation process, *Appl. Surf. Sci.* 253 (2007) 7207–7210.
- [7] A. Prakash, S. Maikap, S.Z. Rahaman, S. Majumdar, S. Manna, S.K. Ray, Resistive switching memory characteristics of Ge/GeO_x nanowires and evidence of oxygen ion migration, *Nanoscale Res. Lett.* 8 (2013) 220.
- [8] P. Hidalgo, E. Liberti, Y.R. Lazzano, B. Méndez, J. Piqueras, GeO_2 Nanowires Doped with Optically Active Ions, *J. Phys. Chem. C* 113 (2009) 17200–17205.
- [9] X.L. Wang, W.Q. Han, H. Chen, J. Bai, T.A. Tyson, X.Q. Yu, X.J. Wang, X.Q. Yang, Amorphous Hierarchical Porous GeO_x as High-Capacity Anodes for Li Ion Batteries with Very Long Cycling Life, *J. Am. Chem. Soc.* 133 (2011) 20692–20695.
- [10] A. Ghosh, P. Guha, S. Mukherjee, R. Bar, Growth of Au capped GeO_2 nanowires for visible-light photodetection, *Appl. Phys. Lett.* 109 (2016) 123105.
- [11] Y. Sun, W. Xu, X. Fu, Z. Sun, J. Wang, J. Zhang, D. Rosenbach, R. Qi, K. Jiang, C. Jing, Z. Hu, X. Mab, J. Chua, Evaluation of lattice dynamics, infrared optical properties and visible emissions of hexagonal GeO_2 films prepared by liquid phase deposition, *J. Mater. Chem. C* 5 (48) (2017) 12792–12799.
- [12] M.S. Rathore, A. Vinod, R. Angalakurthi, A.P. Pathak, S.K. Thatikonda, S.R. Nelamarri, Ion beam modification of structural and optical properties of GeO_2 thin films deposited at various substrate temperatures using pulsed laser deposition, *Appl. Phys. A-Mater.* 123 (11) (2017) 1–10.
- [13] M.S. Rathore, A. Vinod, N.S. Rao, Structural and Optical Properties of GeO_2 Thin Films Prepared by E-Beam Evaporation, *J. Comput. Theor. Nanos.* 22 (11) (2016) 3798–3801.

- [14] S.H. Wemple, M. DiDomenico, Behavior of the electronic dielectric constant in covalent and ionic materials, *Phys. Rev. B* 3 (1971) 1338.
- [15] S.H. Wemple, M. DiDomenico, Optical dispersion and the structure of solids, *Phys. Rev. Lett.* 23 (1969) 1156.
- [16] E. Şenadım Tüzemen, H. Kavak, R. Esen, Influence of oxygen pressure of ZnO/glass substrate produced by pulsed filtered cathodic vacuum arc deposition, *Phys. B Condensed Matter* 390 (2007) 366–372.
- [17] C.V. Ramana, G. Carbajal-Franco, R.S. Vemuri, I.B. Troitskaia, S.A. Gromilov, V.V. Atuchin, Optical properties and thermal stability of germaniumoxide (GeO₂) nanocrystals with α -quartz structure, *Mater. Sci. Eng. B* 174 (2010) 279–284.
- [18] X.Y. Wang, L. Duan, G.F. Dong, P. Wei, W. Wang, Y.Qiu L.Wang, Synthesis and characterization of nano/microstructured crystalline germanium dioxide with novel morphology, *Chin. Sci. Bull.* 54 (16) (2009) 2810–2813.
- [19] T. Lange, W. Njoroge, H. Weis, M. Beckers, M. Wuttig, Physical properties of thin GeO₂ films produced by reactive DC magnetron sputtering, *Thin Solid Films* 365 (1) (2000) 82–89.
- [20] D.K. Takci, E. Senadım Tuzemen, K. Kara, S. Yılmaz, R. Esen, Ö. Bağlayan, Influence of Al concentration on structural and optical properties of Al-doped ZnO thin films, *J. Mater. Sci. Mater Electron.* 25 (5) (2014) 2078–2085.
- [21] F. Yakuphanoglu, Electrical characterization and device characterization of ZnO microring shaped films by sol-gel method, *J. Alloy Compd.* 507 (1) (2010) 184–189.
- [22] S. Mobtakeri, Y. Akaltun, A. Ozer, M. Kılıç, E. Senadım Tüzemen, E. Gür, Gallium oxide films deposition by RF magnetron sputtering; a detailed analysis on the effects of deposition pressure and sputtering power and annealing, *Ceram. Int.* 47 (2) (2021) 1721–1727.
- [23] C.V. Ramana, E.J. Rubio, C.D. Barraza, A.M. Gallardo, S.A. McPeak, S. Kotru, J.T. Grant, Chemical bonding, optical constants, and electrical resistivity of sputter deposited gallium oxide thin films, *J. Appl. Phys.* 115 (4) (2014) 043508.
- [24] T.N. Nunley, N.S. Fernando, N. Samarasingha, J.M. Moya, C.M. Nelson, A.A. Medina, S. Zollner, Optical constants of germanium and thermally grown germanium dioxide from 0.5 to 6.6 eV via a multi-sample ellipsometry investigation, *J. Vac. Sci. Technol. B* 34 (6) (2016) 061205.
- [25] E. Senadım Tuzemen, S. Eker, H. Kavak, R. Esen, Dependence of film thickness on the structural and optical properties of ZnO thin films, *Appl. Surf. Sci.* 255 (12) (2009) 6195–6200.

The power of the Web of Science™ on your mobile device, wherever inspiration strikes.

Dismiss

Learn More


Already have a manuscript?

Use our Manuscript Matcher to find the best relevant journals!

Find a Match

Filters

Clear All

Web of Science Coverage 

Open Access  

Category 

Country / Region 

Language 

Frequency 

Journal Citation Reports 

Refine Your Search Results

Journal of Molecular Structure

Search

Sort By: Relevancy 

Search Results

Found 960 results (Page 1)

[Share These Results](#)

Exact Match Found

JOURNAL OF MOLECULAR STRUCTURE

Publisher: ELSEVIER , RADARWEG 29, AMSTERDAM, Netherlands, 1043 NX

ISSN / eISSN: 0022-2860 / 1872-8014

Web of Science Core Collection: Science Citation Index Expanded

Additional Web of Science Indexes: Current Contents Physical, Chemical & Earth Sciences | Essential Science Indicators

[Share This Journal](#)

[View profile page](#)

* Requires free login.

Other Possible Matches

NATURE STRUCTURAL & MOLECULAR BIOLOGY

Publisher: NATURE PORTFOLIO , HEIDELBERGER PLATZ 3, BERLIN, Germany, 14197

ISSN / eISSN: 1545-9993 / 1545-9985

Web of Science Core Collection: Science Citation Index Expanded

Additional Web of Science Indexes: Biological Abstracts | BIOSIS Previews | Current Contents Life Sciences | Essential Science Indicators

[Share This Journal](#)

[View profile page](#)

* Requires free login.

ALGORITHMS FOR MOLECULAR BIOLOGY

OPEN ACCESS

Publisher: BMC , CAMPUS, 4 CRINAN ST, LONDON, ENGLAND, N1 9XW

5



ISSN / eISSN: 1748-7188

Web of Science Core Collection: Science Citation Index Expanded

Additional Web of Science Indexes: Biological Abstracts | BIOSIS Previews | Essential Science Indicators

[Share This Journal](#)

[View profile page](#)

* Requires free login.

FRONTIERS IN MOLECULAR BIOSCIENCES

OPEN ACCESS

Publisher: FRONTIERS MEDIA SA , AVENUE DU TRIBUNAL FEDERAL 34, LAUSANNE, SWITZERLAND, CH-1015

ISSN / eISSN: 2296-889X

Web of Science Core Collection: Science Citation Index Expanded

Additional Web of Science Indexes: Biological Abstracts | BIOSIS Previews | Essential Science Indicators

[Share This Journal](#)

[View profile page](#)

* Requires free login.

AIMS MOLECULAR SCIENCE

OPEN ACCESS

Publisher: AMER INST MATHEMATICAL SCIENCES-AIMS , PO BOX 2604, SPRINGFIELD, United States, MO, 65801-2604

ISSN / eISSN: 2372-0301

Web of Science Core Collection: Emerging Sources Citation Index

[Share This Journal](#)

[View profile page](#)

* Requires free login.

AMERICAN JOURNAL OF RESPIRATORY CELL AND MOLECULAR BIOLOGY

Publisher: AMER THORACIC SOC , 25 BROADWAY, 18 FL, NEW YORK, USA, NY, 10004

ISSN / eISSN: 1044-1549 / 1535-4989

Web of Science Core Collection: Science Citation Index Expanded

Additional Web of Science Indexes: Biological Abstracts | BIOSIS Previews | Current Contents Life Sciences | Essential Science Indicators

[Share This Journal](#)

[View profile page](#)

* Requires free login.

BIOCHEMISTRY AND MOLECULAR BIOLOGY EDUCATION

Publisher: WILEY , 111 RIVER ST, HOBOKEN, USA, NJ, 07030-5774

ISSN / eISSN: 1470-8175 / 1539-3429

Web of Science Core Collection: Science Citation Index Expanded



Additional *Web of Science* Indexes: **Essential Science Indicators**

[Share This Journal](#)

[View profile page](#)

* Requires free login.

BIOCHIMICA ET BIOPHYSICA ACTA-MOLECULAR AND CELL BIOLOGY OF LIPIDS

Publisher: **ELSEVIER , RADARWEG 29, AMSTERDAM, Netherlands, 1043 NX**

ISSN / eISSN: **1388-1981 / 1879-2618**

Web of Science Core Collection: **Science Citation Index Expanded**

Additional *Web of Science* Indexes: **Biological Abstracts | BIOSIS Previews | Current Contents Life Sciences | Essential Science Indicators**

[Share This Journal](#)

[View profile page](#)

* Requires free login.

BIOCHIMICA ET BIOPHYSICA ACTA-MOLECULAR BASIS OF DISEASE

Publisher: **ELSEVIER , RADARWEG 29, AMSTERDAM, Netherlands, 1043 NX**

ISSN / eISSN: **0925-4439 / 1879-260X**

Web of Science Core Collection: **Science Citation Index Expanded**

Additional *Web of Science* Indexes: **Biological Abstracts | BIOSIS Previews | Current Contents Life Sciences | Essential Science Indicators**

[Share This Journal](#)

[View profile page](#)

* Requires free login.

BIOCHIMICA ET BIOPHYSICA ACTA-MOLECULAR CELL RESEARCH

Publisher: **ELSEVIER , RADARWEG 29, AMSTERDAM, Netherlands, 1043 NX**

ISSN / eISSN: **0167-4889 / 1879-2596**

Web of Science Core Collection: **Science Citation Index Expanded**

Additional *Web of Science* Indexes: **Biological Abstracts | BIOSIS Previews | Current Contents Life Sciences | Essential Science Indicators**

[Share This Journal](#)

[View profile page](#)

* Requires free login.

Items per page: 10 ▾ 1 – 10 of 960 < > >>

standards. The views and opinions expressed in any journal are those of the author(s) and do not necessarily reflect the views or opinions of Clarivate. Clarivate remains neutral in relation to territorial disputes, and allows journals, publishers, institutes and authors to specify their address and affiliation details including territory.

Criteria for selection of newly submitted titles and re-evaluation of existing titles in the Web of Science are determined by the Web of Science Editors in their sole discretion. If a publisher's editorial policy or business practices negatively impact the quality of a journal, or its role in the surrounding literature of the subject, the Web of Science Editors may decline to include the journal in any Clarivate product or service. The Web of Science Editors, in their sole discretion, may remove titles from coverage at any point if the titles fail to maintain our standard of quality, do not comply with ethical standards, or otherwise do not meet the criteria determined by the Web of Science Editors. If a journal is deselected or removed from coverage, the journal will cease to be indexed in the Web of Science from a date determined by the Web of Science Editors in their sole discretion – articles published after that date will not be indexed. The Web of Science Editors' decision on all matters relating to journal coverage will be final.

Clarivate.™ Accelerating innovation.

© 2023 Clarivate

[Legal center](#)

[Privacy notice](#)

[Cookie policy](#)

[Tanımlama Bilgisi Ayarları](#)

[Copyright notice](#)

[Help](#)

